

Energy relaxation dynamics in the optical excited state of myoglobin

Hiroshi Murakami and Takashi Kushida

Department of Physics, Faculty of Science, Osaka University, Toyonaka, Osaka 560, Japan

(Received 17 August 1995; revised manuscript received 18 January 1996)

In order to obtain information on the fast dynamics of the conformational fluctuation of a protein, absorption, steady-state, and time-resolved fluorescence spectra have been measured in the spectral region of the lowest optical absorption band of Zn-substituted myoglobin between 170 and 290 K. The obtained spectra have been analyzed using the single-site spectra calculated from the experimentally determined effective density of states of vibrational modes of Zn-substituted myoglobin. A configuration-coordinate model has been adopted to take into account the inhomogeneous broadening of the spectra. The fluorescence spectrum has also been compared with that calculated from the absorption spectrum on the basis of the Einstein relation. The results of the analyses show that the conformational relaxation occurs in the excited state, but is not completed within the lifetime of the excited state even at room temperature. The dynamic Stokes shift, which is expected in such a case, has not been observed in the whole temperature range examined. This indicates that the excited-state dynamics in myoglobin is different from that due to the thermal crossing over static potential barriers. The experimental results are explained well by a model based on hierarchically constrained dynamics. [S0163-1829(96)02226-6]

I. INTRODUCTION

Recently, there has been a growing interest in complex systems such as glassy materials. In particular, much attention has been focused, in recent years, on the relaxation dynamics. The conformational fluctuation of a protein is considered to be important not only from the viewpoint of biological functions, but also as a typical example of the fluctuation of a complex system. It is known that a protein molecule has a large number of conformational substates, i.e., nearly degenerate local minima of the free energy, because of its complexity and flexibility.¹ Proteins in different substrates have the same coarse structure and almost the same energy. Microscopically, however, they have slightly different structures and accordingly slightly different energies. Conformational fluctuation corresponds to the transition among the substates. At physiological temperatures, the protein molecule is considered to fluctuate among the conformational substates and behave like a liquid. At low temperatures, on the other hand, it will freeze into some substate and become glasslike. Such a picture of proteins has been verified mainly in myoglobin by various methods, such as x-ray structure analysis,²⁻⁴ Mössbauer spectroscopy,⁵⁻¹⁰ specific-heat measurements,¹¹⁻¹³ and incoherent neutron scattering.^{14,15}

There have been several investigations on the glasslike dynamics of proteins.¹⁶ For example, the time profile of the binding kinetics of ligands such as oxygen and carbon monoxide bound to myoglobin, after photodissociation, has been found to be nonexponential at temperatures lower than 160 K and to be reproduced well by a sum of exponential functions with different time constants that obey the Arrhenius expression.¹⁷ The temperature-independent distribution function of the barrier height for the ligand binding has also been determined. Further, it has been shown that this distribution is not due to an intrinsically nonexponential kinetics within a single protein molecule, but due to parallel dynamics of pro-

tein molecules with different time constants, i.e., an ensemble heterogeneity. Moreover, from the investigations of the relaxation processes to the deoxy equilibrium structure after photodissociation of myoglobin, it has been suggested that the conformational substate shows a hierarchical glasslike structure.¹⁸

Myoglobin has several absorption bands in the visible region due to the optical transitions in a chromophore of protoheme (Fe-protoporphyrin IX), which is packed by the polypeptide chain. Since the conformational change affects the optical spectra, it is possible to study the conformational fluctuation of a protein by optical spectroscopy using this chromophore as a probe. In fact, from the temperature dependence of the spectral shape of the Soret band of deoxymyoglobin, it has been shown that the absorption spectrum above ~ 250 K is reproduced under the assumption of the thermal equilibrium of the protein molecule in the ground state, while that below ~ 250 K is insensitive to temperature and can be explained by assuming the Boltzmann distribution at 250 K.¹⁹ This result suggests that deoxymyoglobin becomes glasslike below ~ 250 K. Although the glass transition temperature thus estimated is a little higher than that of 160–220 K obtained in myoglobin by other methods, the glass transition temperature is sensitive to the water content of the sample¹³ and may also depend on the myoglobin species. It is also possible that only the fluctuation among substates with high potential barrier heights affects the optical spectrum. Further, the broad homogeneous width of the absorption band due to the very short excited-state lifetime in deoxymyoglobin may have obscured the transition temperature in this experiment.

Time-resolved fluorescence spectroscopy is considered to be very effective for obtaining information on the fast conformational relaxation. Reflecting the fact that a protein has many conformational substates, the adiabatic potential surfaces of the ground and excited states of the chromophore are considered to have a large number of energy valleys, as il-

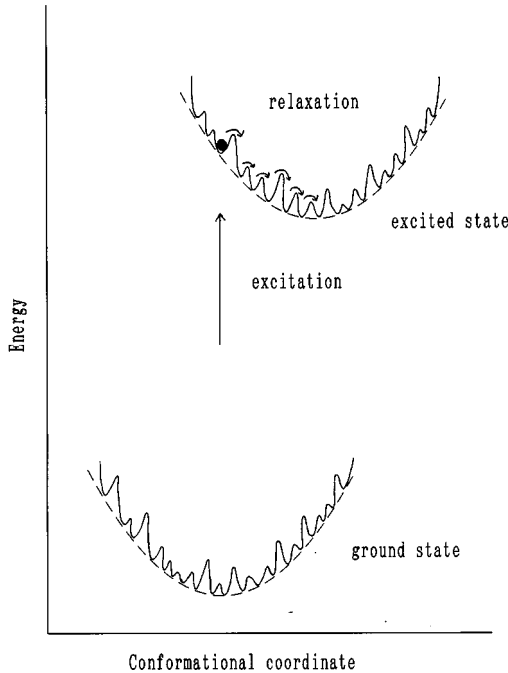


FIG. 1. Adiabatic potential curves (solid lines) of the electronic ground and excited states of a protein as a function of the conformational coordinate, where the local minima indicate the conformational substates. The dashed lines correspond to the configuration-coordinate model represented by Eqs. (3) and (4).

illustrated schematically in Fig. 1. According to the Franck-Condon principle, the optical transition occurs vertically in this figure. After the protein is excited by light irradiation, it may go down toward the bottom of the potential surface in the excited state during the fluorescence process, as seen in Fig. 1. Therefore, information on the rapid relaxation process in the excited state will be contained directly in the time-resolved fluorescence spectra. In fact, it is known in dye solutions that the time-dependent change in the fluorescence spectrum gives detailed information on the excited-state relaxation dynamics.^{20,21} If the protein is liquid-like at high temperatures, it may show fluorescence characteristics similar to those of dye solutions. Consequently, it will be possible to obtain information on the fluctuation among the conformational substates of a protein from the relaxation dynamics in the excited state by the fluorescence spectroscopy. Although there have been low-temperature experiments such as fluorescence line-narrowing spectroscopy,²² the detailed fluorescent characteristics of myoglobin have not been studied yet in the liquidlike temperature range.

In order to investigate the relaxation among the conformational substates in the excited state of a protein, we have measured absorption spectra, time-resolved laser-induced fluorescence (TRF) spectra and stationary-laser-excited fluorescence (SEF) spectra in the temperature range between about 170 K, the vitrification temperature of the solvent, and room temperature in Zn-substituted myoglobin, i.e., myoglobin whose heme iron is replaced with zinc. This substitution is necessary because native myoglobin shows no fluorescence. Efficient fluorescence due to the $Q(0,0)$ transition is observed in the red spectral region in the case of Zn-substituted myoglobin. Thus we have focused our attention

on the $Q(0,0)$ band, i.e., the lowest optical absorption band, which is due to the transition of a π electron in the porphyrin ring of the chromophore. A part of the result has already been reported briefly.²³

II. THEORETICAL BACKGROUND

When a dye molecule is introduced into disordered systems such as solutions and polymers, the configuration of the surroundings of the dye molecule is not uniform. Each configuration of the surroundings is called a site. In the case of a chromoprotein that can have various conformations, the chromophore corresponds to the dye, while a conformational substate to a site. Since the transition energy depends on the site, the optical spectra exhibit inhomogeneous broadening when a system has many sites. Then, the absorption spectrum is expressed as

$$I^{\text{ab}}(\omega) = \int_0^\infty G(\omega_0) \omega f^{\text{ab}}(\omega, \omega_0) d\omega_0, \quad (1)$$

where $\omega f^{\text{ab}}(\omega, \omega_0)$ is the absorption spectrum of the dye molecule in a single site with the energy of the zero-phonon line at ω_0 and $f^{\text{ab}}(\omega, \omega_0)$ is called the shape function of the single-site absorption spectrum. Further, $G(\omega_0)$ is the site-energy distribution function, which describes the inhomogeneous broadening. If no site change occurs in the excited state, the SEF spectrum measured by a photon-counting method under monochromatic light excitation is expressed as

$$I^{\text{SEF}}(\omega, \omega_l) = \int_0^\infty G(\omega_0) \omega_l f^{\text{ab}}(\omega_l, \omega_0) \omega^3 f^{\text{fl}}(\omega, \omega_0) d\omega_0, \quad (2)$$

where ω_l is the excitation energy and $\omega^3 f^{\text{fl}}(\omega, \omega_0)$ is the single-site photon-number fluorescence spectrum. In this paper, we employ the configuration-coordinate (CC) model in the treatment of the inhomogeneous broadening and the single-site spectra are calculated from the experimentally obtained effective density of states of vibrational modes of Zn-substituted myoglobin.

A. Configuration-coordinate model

It has been shown that the CC model is successful in explaining the inhomogeneously broadened line shapes of the chromophore in deoxymyoglobin and dyes in solutions.^{19,24} In this model, the energies of the local minima of the adiabatic potential surfaces for the ground and excited electronic states of a chromophore or a dye interacting with the surroundings are assumed to be on the smooth curves of functions of the configuration coordinate Q , which corresponds to the conformation of a protein or the configuration of the surroundings (Fig. 1). We assume these curves to be parabolas with the same curvature and different minimum positions as

$$U_e(Q) = a(Q - Q_0)^2 + E', \quad (3)$$

$$U_g(Q) = aQ^2. \quad (4)$$

These curves correspond to the envelopes of the energies of the conformational substates, which are assumed to be dis-

tributed uniformly on the curves. Then, the site-energy distribution function $G(\omega_0)$ is derived using the population distribution in the ground state $P(Q)$ through

$$G(\omega_0) = \int_{-\infty}^{+\infty} P(Q) \delta[\omega_0 - \Delta U(Q)] dQ, \quad (5)$$

with

$$\begin{aligned} \Delta U(Q) &= U_e(Q) - U_g(Q) = -2aQ_0Q + E, \\ (E &= E' + aQ_0^2 \equiv E' + d/2), \end{aligned} \quad (6)$$

where d is the Stokes shift for the case that the thermalization is sufficiently fast in both the ground and excited states. If $P(Q)$ is a Boltzmann distribution, we have

$$\begin{aligned} G(\omega_0) &\propto \int_{-\infty}^{+\infty} \exp\left(-\frac{aQ^2}{k_B T}\right) \delta[\omega_0 - \Delta U(Q)] dQ, \\ &\propto \exp\left[-\frac{(\omega_0 - E)^2}{2dk_B T}\right], \end{aligned} \quad (7)$$

where k_B is the Boltzmann constant and T is the absolute temperature.

In this CC model, the energy relaxation in an electronic state accompanied by the change in the configuration of the surroundings or the conformation is interpreted in terms of the population dynamics on the potential curve. Time-dependent changes of the TRF and transient hole-burning spectra of dye-solution systems have been explained very well by using this model.^{20,21,25}

B. Weighted density of states of vibrational modes

The single-site absorption spectrum broadens because of the coupling of the electron of the chromophore with the vibrations of the atoms constituting the chromophore and its surroundings and contains a phonon sideband in addition to the zero-phonon line. If we employ the adiabatic and Condon approximations, the absorption spectrum can be expressed using vibrational wave functions for the cases that the chromophore is in the ground and excited states. Let us regard the motions of the atoms as an ensemble of normal-mode harmonic oscillators and confine ourselves to the case of the linear interaction between these oscillators and the electron involved in the optical transition. Then, we can calculate these wave functions and accordingly the absorption spectrum analytically.²⁶ The result is expressed using the density of states of vibrational modes weighted by the electron-vibration coupling strength. This weighted density of states of vibrational modes (WDOS) is given by

$$s(\nu) = \sum_{\lambda} \xi_{\lambda}^2 \delta(\nu - \nu_{\lambda}), \quad (8)$$

where ξ_{λ} is the dimensionless coupling constant between the electron and the vibrational mode λ with energy ν_{λ} .

Using the occupation number $n_T(\nu)$ of the phonon with energy ν , let us define the phonon function corresponding to the one-phonon sideband component of the absorption spectrum as

$$g(\nu) = [n_T(\nu) + 1]s(\nu) + n_T(-\nu)s(-\nu). \quad (9)$$

Then, the shape function of the single-site absorption spectrum is expressed as

$$f^{\text{ab}}(\omega, \omega_0) = \delta(\omega - \omega_0) + \sum_{m=1}^{\infty} \Phi^{(m)}(\omega, \omega_0), \quad (10)$$

with

$$\begin{aligned} \Phi^{(m)}(\omega, \omega_0) &= (1/m!) \int \int \cdots \int g(\nu_1)g(\nu_2)\cdots g(\nu_m) \\ &\quad \times \delta(\omega - \omega_0 - \nu_1 - \nu_2 - \cdots - \nu_m) \\ &\quad \times d\nu_1 d\nu_2 \cdots d\nu_m, \end{aligned} \quad (11)$$

where the δ -function component corresponds to the zero-phonon line, while $\Phi^{(m)}(\omega, \omega_0)$ to the m -phonon sideband component ($m=1, 2, \dots$). Since the mirror symmetry relation holds between the shape functions of the absorption and fluorescence spectra under the above assumptions, we obtain

$$f^{\text{ab}}(\omega, \omega_0) = f^{\text{fl}}(2\omega_0 - \omega, \omega_0). \quad (12)$$

Further, if these shape functions, and accordingly the WDOS, are independent of the site, we have $f(\omega, \omega_0) = f(\omega - \omega_0)$ and the following relation holds:

$$f^{\text{ab}}(\omega - \omega_0) = f^{\text{fl}}(\omega_0 - \omega). \quad (13)$$

Thus once the WDOS is obtained, we can derive the single-site absorption and fluorescence spectra at a given temperature.

Recently, a method to determine the WDOS and the site-energy distribution function in a dye-polymer system has been devised using a fluorescence line-narrowing technique.^{27,28} The single-site spectra have been obtained for a dye in polymer films by the above-mentioned procedure from thus determined WDOS's. It has been shown that the SEF spectra calculated using these data through Eq. (2) reproduce the spectra measured at various temperatures.²⁸ In Sec. V we use the single-site spectra calculated from the WDOS obtained in myoglobin.

III. EXPERIMENTAL PROCEDURE

In order to prepare Zn-substituted myoglobin, the Fe-protoporphyrin IX in myoglobin was replaced with Zn-protoporphyrin IX. The structural formula of Zn-protoporphyrin IX is known to be the same as that of Fe-protoporphyrin IX, except that the Fe ion in the center of protoporphyrin IX is replaced with a Zn ion.²⁹ The detailed procedure of preparation has already been described.²² In order to prevent the sample from becoming opaque with decreasing temperature, Zn-substituted myoglobin in a glycerol-buffer solution (volume ratio of 2:1), which we call ZnMb hereafter, was used. For the purpose of comparison of ZnMb with a solution containing the same chromophore, Zn-protoporphyrin IX (Porphyrin Products Inc.) in *N,N*-dimethylformamide (DMF; Nacalai Tesque Inc.), was prepared. The sample in a quartz cuvette with a 1 mm path length was placed in a flow-type cryostat and cooled by the continuous flow of gas from a liquid-nitrogen vessel. The

sample temperature was maintained within ± 1 K during the measurement by a temperature controller (Omron E5EX).

It is known that a double bond in a molecule possibly reacts with oxygen by light irradiation and breaks into a single bond. The porphyrin dye is a conjugated system containing several double bonds. Therefore, oxygen in ZnMb and Zn-protoporphyrin IX in DMF was exchanged for nitrogen by bubbling nitrogen gas into the sample and then the sample cell was hermetically sealed. These processes were performed in a glove bag. Even if the reaction occurs with residual oxygen, it has no problem for our experiment because the absorption spectrum of the reacted molecule is located far from the spectral region of our measurement.

The TRF spectra were measured by a time-correlated single-photon counting method under excitation by a rhodamine 6G laser pumped by a cw mode-locked Ar⁺ laser (Spectra Physics model 2020). The whole experimental system has already been described in detail.³⁰ The instrumental response function to the laser pulse was found to have a half-width at half maximum of about 100 ps. The TRF spectra were recorded using a time gate of 300 ps width, which was obtained by a time-to-amplitude converter equipped with a single-channel analyzer. The absorption and SEF spectra were measured by a combination of a cooled side-on-type photomultiplier (Hamamatsu Photonics model R928) and a double monochromator (Spex model 14018). The light sources for the measurements of the absorption and SEF spectra were a halogen lamp and a rhodamine 6G laser pumped by a cw Ar⁺ laser, respectively. The intensity of the dye laser beam was stabilized by a laser power controller (Cambridge Research and Instrumentation model LPC-VIS).

The obtained fluorescence spectra were corrected for the wavelength-dependent transmittance of the monochromator and sensitivity of the detector. Further, in order to obtain the shape functions, the absorption and fluorescence spectra were divided by ω and ω^3 , respectively, where ω is the energy of the detected photon.

IV. EXPERIMENTAL RESULTS

The dotted lines in Fig. 2 show the temperature dependence of the absorption spectrum of ZnMb. The peak energy shifts toward the low-energy side and the width broadens with increasing temperature. It was found that the fluorescence spectrum depends on the excitation wavelength up to room temperature. As an example, the excitation-energy dependence of the SEF spectrum at 293 K is depicted in Fig. 3. We see that the peak energy of the fluorescence spectrum shifts toward the high-energy side with a slight increase of the width, as the excitation energy is increased. Next, we show the temperature dependence of the SEF spectrum by dotted lines in Fig. 4. It is noticed that its peak energy shifts toward the low-energy side and its width broadens with increasing temperature. Finally, the TRF spectra at various temperatures are shown in Fig. 5. Almost no time-dependent change of the spectrum is observed after 400 ps at each temperature. Further, the spectral width and also the difference between the peak energy and the excitation energy increase with increasing temperature. It should be noted that the relaxation from the excitation energy to the observed peak energy occurs within 400 ps. In the whole temperature region

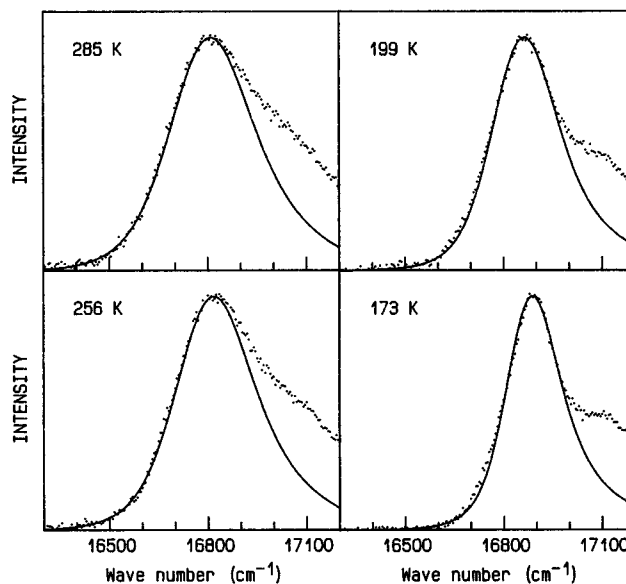


FIG. 2. Temperature dependence of the absorption spectrum of ZnMb (dotted lines). The solid lines were obtained from Eq. (1) by using the single-site absorption spectrum calculated from the weighted density of states of vibrational modes (WDOS) and the site-energy distribution function of Eq. (7).

between 170 and 290 K, the time profile of the fluorescence intensity was almost independent of both observation wavelength and temperature and was essentially in accordance with the single exponential function with a time constant of 2.1 ns, though the time profile just after the excitation was not measurable at the excitation wavelength owing to the strong scattering of the laser light by the sample. The TRF spectra of Fig. 5 are essentially the same as the SEF spectra. This is reasonable if the above relaxation from the excitation energy occurs within a time much shorter than the fluorescent decay time, because the observed TRF spectra are time independent. In the following sections, we discuss these experimental results from several viewpoints.

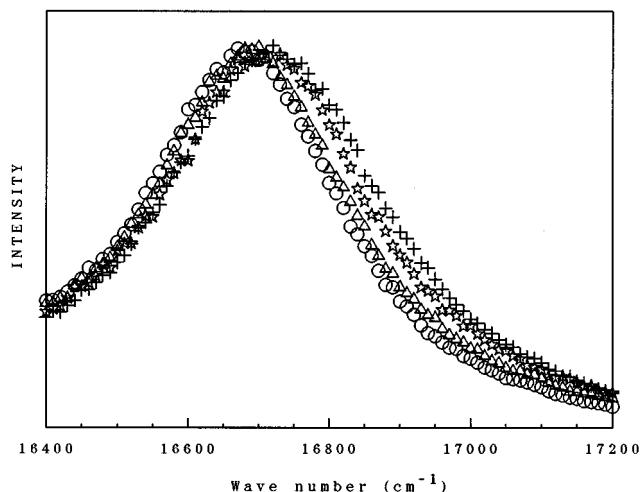


FIG. 3. Stationary laser-excited fluorescence (SEF) spectra of ZnMb excited at 16 900 (crosses), 16 800 (stars), 16 700 (triangles), and 16 600 cm^{-1} (circles) at 293 K.

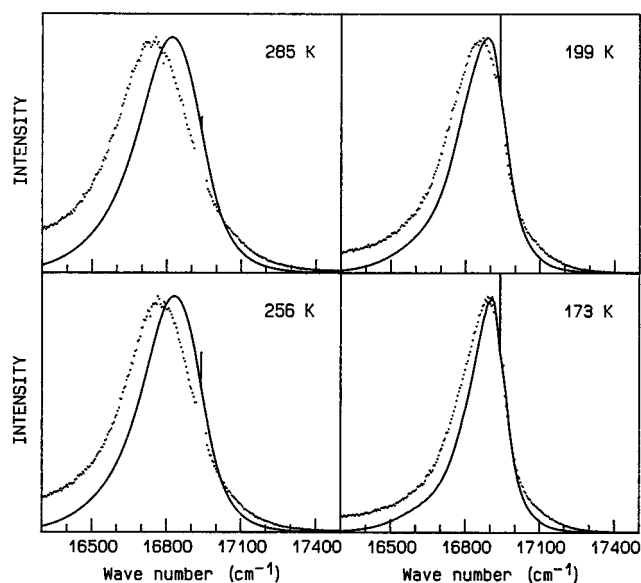


FIG. 4. Temperature dependence of the SEF spectrum of ZnMb excited at $16\,940\text{ cm}^{-1}$ (dotted lines). The solid lines were obtained from Eq. (2) by using the site-energy distribution function of Eq. (7) and the single-site absorption and fluorescence spectra calculated from the WDOS.

V. DISCUSSION AND ANALYSIS

A. Existence of two relaxation modes

The SEF spectrum of ZnMb is dependent on the excitation energy. Therefore, it is clear that there exists an inhomogeneous broadening mechanism of the absorption spec-

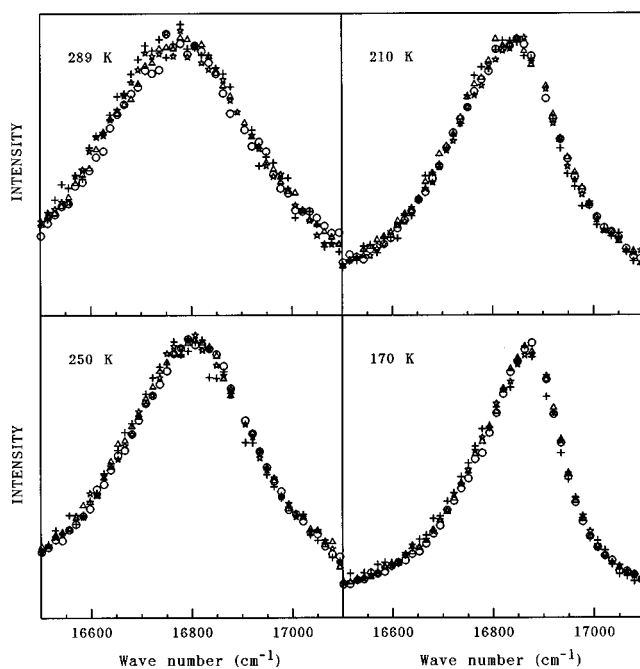


FIG. 5. Temperature dependence of the time-resolved fluorescence (TRF) spectra of ZnMb at 0.4 (circles), 1 (triangles), 2 (stars), and 4 (crosses) ns after the excitation. The exciting laser wave number was $16\,890\text{ cm}^{-1}$.

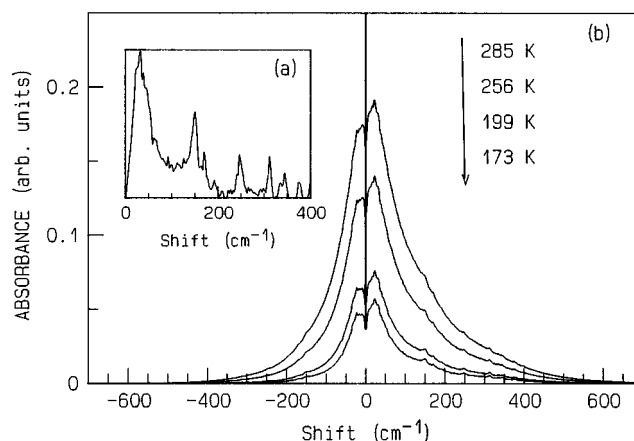


FIG. 6. (a) WDOS of ZnMb (Ref. 22) and (b) temperature dependence of the single-site absorption spectrum calculated from the WDOS through Eq. (10) using Eqs. (9) and (11). The spectra are normalized at the peak of the zero-phonon line, which has been assumed to have a width (FWHM) of 1 cm^{-1} .

trum. It is ascribed to the presence of many conformational substates in myoglobin. As shown later, the analysis of the absorption spectrum indicates that the population in the ground state is in thermal equilibrium at all the temperatures examined. Therefore, the conformational fluctuation among the substates is considered to occur in this temperature range. However, the relaxation connected with this fluctuation in the excited state is concluded to have a time scale much longer than the excited-state lifetime, because almost no time-dependent change is observed in the TRF spectrum after 400 ps and also because the SEF spectrum depends on the excitation wavelength. On the other hand, since the peak shift of the TRF spectrum from the excitation energy occurs within the temporal resolution of our measurement, there is a relaxation process that finishes within a few hundred picoseconds. Thus ZnMb has at least two relaxation modes with different time scales. In dye solutions also, it has been found that there are two relaxation modes.^{20,21} In this paper, we are concerned with the fast relaxation mode in ZnMb.

The peak energy of the SEF spectrum shifts with temperature. However, since the absorption spectrum also shifts in a similar way with temperature, it is not clear whether the temperature-dependent shift of the SEF spectrum is related to some relaxation process among the conformational substates in the excited state or is due to the same origin as that of the absorption spectrum. Hence we first determine the parameters of the CC model from the analysis of the temperature dependence of the absorption spectrum and then analyze the SEF spectrum using the determined parameters.

B. Analysis of the absorption spectra using the CC model and WDOS

Recently, Ahn, Kanematsu, and Kushida²² have obtained the WDOS of ZnMb by a fluorescence line-narrowing technique at 4 K as shown in Fig. 6(a). This WDOS is considered to be independent of the conformational substate, because the laser-induced fluorescence spectrum calculated under this assumption reproduces the spectra excited at various wavelengths. Therefore, we can calculate the single-site absorp-

tion spectrum at a given temperature through Eq. (10) using Eqs. (9) and (11), when the temperature dependence of the WDOS is negligible. The obtained spectra are shown in Fig. 6(b). Employing Eq. (7) for the site-energy distribution function with two fitting parameters d and E , we calculate the absorption spectra through Eq. (1), where we assume that the population in the ground state is thermalized and also that the transition probability is insensitive to Q . The spectral broadening due to the lifetime of the excited state and the spectral resolution of the monochromator is neglected, because it is small enough compared with the width of the absorption spectrum.

As seen in Fig. 2, the calculated spectra reproduce the measured ones very well except for the high-energy region, where another band is present. This band may be attributed to the transition from the ground state of the chromophore to the upper level of the two excited levels split by the Jahn-Teller effect.²⁹ The good agreement between the experiment and calculation in Fig. 2 indicates that the Boltzmann distribution is established in the ground state of ZnMb in the temperature region of our experiment. Further, from the result, the neglect of the temperature dependence of the WDOS is considered to be a good approximation. This is also supported by the fact that the laser-induced fluorescence spectra of dye-doped polymers at various temperatures are reproduced well using the WDOS obtained at 4 K.²⁸ From the fitting, d was determined to be $\sim 37 \text{ cm}^{-1}$, while E was found to change from 16 875 to 16 790 cm^{-1} with increasing temperature. At least a part of this energy shift is considered to originate from the temperature-dependent change of the refractive index of the solvent.³¹

C. Analysis of the laser-induced fluorescence spectra using the CC model and WDOS

In this section, we simulate the SEF spectra using Eq. (2) on the basis of the CC model, assuming that no relaxation occurs among the conformational substates in the excited state. It should be noted that even if there is no jump among the substates, the fast energy relaxation may be explained by the relaxation due to the vibrational degrees of freedom of a protein, i.e., by the slight changes in the equilibrium positions of the atoms.^{32,33} In our simulation, the parameter values obtained from the analysis of the absorption spectra are employed. Further, we use the single-site fluorescence spectrum calculated from the WDOS of Fig. 6(a). The laser line-width, the spectral broadening due to the finite lifetime of the excited state, and the spectral resolution of the monochromator are neglected, because they are small enough compared to the width of the fluorescence spectrum. The calculated SEF spectra are compared with experiment in Fig. 4.

In the simulated spectra, a spike is present at the excitation energy, owing to the δ -function-like zero-phonon line. However, it has been found that there is no spike in the TRF spectrum, when it is measured with a time gate after the termination of the exciting pulse. Since the measured TRF and SEF spectra are almost identical to each other, the spike is considered to be absent in the SEF spectrum. The explanation for this discrepancy between the simulation and experiment is as follows. Contrary to the above assumptions, there may be a relaxation process among the conformational

substates in the excited state. Then, the molecules excited through the zero-phonon line will be distributed over various substates by the relaxation and the number of the molecules that contribute to the spike will become small. Further, it is considered, as another reason, that the zero-phonon line has a large spectral breadth in this temperature range. Recently, it has been reported in dye-doped polymer films that the zero-phonon line has a considerable breadth at temperatures higher than about 20 K, which is attributed to the quadratic terms in the electron-phonon coupling.²⁸

Even if we neglect the spike, the simulated spectra in Fig. 4 are different from the measured ones in the whole temperature range examined. Further, the difference between the peak energies of the simulated and measured spectra becomes larger with increasing temperature. As for the spectral width, the measured spectrum is broader than the simulated one and the former broadens somewhat faster than the latter with increasing temperature. Moreover, the measured spectra are always located in the low-energy side of the simulated ones. These results are interpreted in terms that the relaxation among the conformational substates occurs in the excited state during the lifetime of the excited state. This interpretation is consistent with the above explanation for the absence of the spike in the SEF spectrum. Since the TRF spectra show almost no time-dependent change after 400 ps over the temperature range examined, the time constant of this relaxation must be much shorter than a few hundred picoseconds. Namely, it is concluded that the peak shift of the TRF spectrum from the excitation energy, which occurs within the temporal resolution of our measurement, is caused not only by the relaxation due to the vibrational degrees of freedom of the protein in a conformational substate but also by the relaxation among the substates. This is in contrast with the case of 4 K, where the SEF spectrum is understood well by assuming that no relaxation among the substates occurs in the excited state within the fluorescent decay time.²² Further, since the difference between the peak energies of the simulated and measured spectra corresponds to the magnitude of the energy relaxation among the substates, it can be said that the conformational relaxation becomes larger with increasing temperature.

D. Analysis of the laser-induced fluorescence spectra based on the Einstein relation

In this section we compare the measured SEF spectra with those obtained under the assumption that the time constant of the relaxation among the conformational substates is much shorter than the lifetime of the excited state. This assumption means that the fluorescence is due to the population in thermal equilibrium in the excited state. Hence we call this fluorescence spectrum an equilibrium-fluorescence (EF) spectrum. No excitation-energy dependence is expected for this spectrum.

When the Boltzmann distribution is established in the ground and excited states before the absorption and fluorescence transitions, the Einstein relation

$$F^{\text{fl}}(\omega) \propto F^{\text{ab}}(\omega) \exp\left[-\frac{\omega}{k_B T}\right] \quad (14)$$

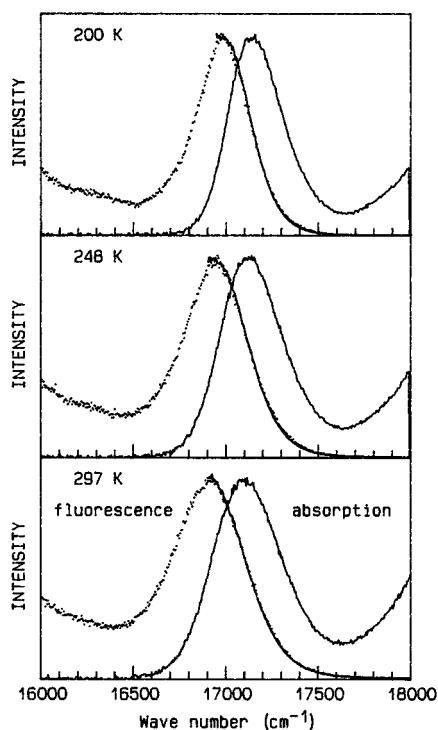


FIG. 7. Temperature dependence of the absorption and SEF spectra of Zn-protoporphyrin IX in DMF. The dotted and solid lines for fluorescence denote the measured spectra and those calculated from the absorption spectra through the Einstein relation, respectively.

holds between the spectral shape functions of the sample, $F^{ab}(\omega)$ and $F^{fl}(\omega)$, for the absorption and fluorescence between the two states.²⁴ Thus, as long as the measured absorption spectrum is due to the population in the thermal equilibrium, we can calculate the EF spectrum from the measured absorption spectrum through Eq. (14). If a reaction occurs in the excited state and the fluorescence is emitted after the system transfers to another state with a different potential, this relation does not hold. Therefore, the Einstein relation requires that no reaction occurs in the excited state.

In Fig. 7 we compare the measured SEF spectrum with the EF spectrum calculated from the absorption spectrum through the Einstein relation in Zn-protoporphyrin IX in DMF. Since the absorbance, and accordingly the signal-to-noise ratio, becomes very small in the low-energy region, the calculation was made only in the high-energy region of the fluorescence spectrum. This sample is a liquid and no excitation-energy dependence of the SEF spectrum was observed in the temperature range of the experiment. Therefore, the populations in the ground and excited states are considered to be in thermal equilibrium before the transitions. In Fig. 7 the fluorescence spectra calculated from the absorption spectra reproduce the measured fluorescence spectra very well. Hence no reaction is considered to occur in the excited state of Zn-protoporphyrin IX in DMF in the temperature region of our experiment.

The band shape of the SEF spectrum of ZnMb is similar to that of the DMF solution. Further, the time profile of the fluorescence intensity of ZnMb is independent of observation wavelength and temperature and almost no deviation from

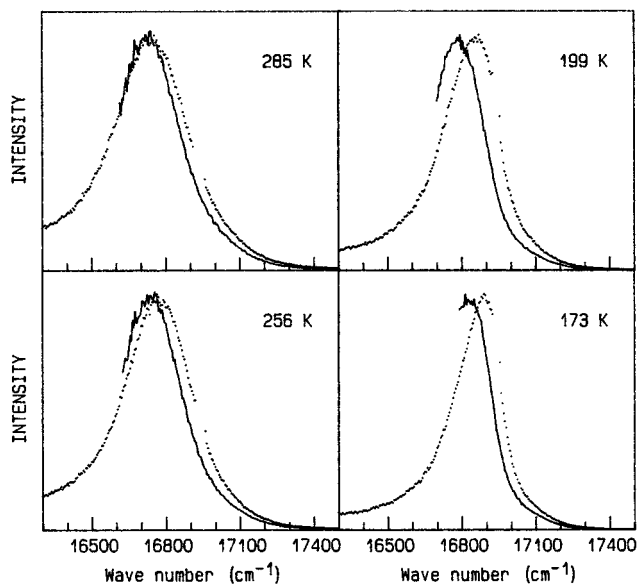


FIG. 8. Temperature dependence of the SEF spectrum of ZnMb. The dotted and solid lines denote the measured spectra and those calculated from the absorption spectra through the Einstein relation, respectively.

the single exponential decay was observed. Therefore, no reaction is considered to occur also in the excited state of ZnMb. As mentioned in Sec. V B, the analysis of the temperature dependence of the absorption spectrum has revealed that ZnMb is in the thermal equilibrium in the ground state in the temperature region of our measurement. Thus it is possible to calculate the EF spectra from the absorption spectra through Eq. (14). The results are shown in Fig. 8 together with the measured SEF spectra. The calculated spectrum is always located in the low-energy side of the measured spectrum and the difference between the energy positions of these spectra becomes larger as temperature is decreased.

We compare the temperature dependence of the peak energies of the measured and simulated SEF and calculated EF spectra of ZnMb in Fig. 9. The peak energy of the SEF

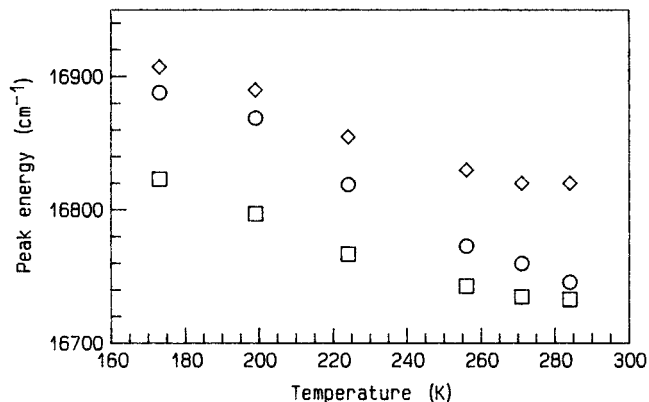


FIG. 9. Temperature dependence of the peak energies of the SEF spectra of ZnMb. The circles, diamonds, and squares denote the peak energies of the measured spectra, the spectra simulated using the WDOS and CC model, and the spectra calculated from the Einstein relation, respectively.

spectrum measured around 170 K is near the peak position due to the population with no relaxation among the conformational substates. However, the measured peak energy shifts toward the peak due to the population in thermal equilibrium as temperature is increased and it is close to the latter at 285 K. Hence we can say that ZnMb is not frozen within a conformational substate in the excited state after the excitation, but relaxes among the substates within a few hundred picoseconds. Further, the magnitude of the relaxation becomes larger with increasing temperature, while the thermal equilibrium is not established in the excited state within the lifetime even at room temperature, as clearly seen from the result in Fig. 3.

E. Comparison with the results in dye solutions

In the case of rhodamine 6G in ethanol-methanol mixture (volume ratio 4:1), we obtained the following results. At room temperature, the measured SEF and calculated EF spectra are essentially identical to each other. However, the difference between the two becomes apparent around 160 K and increases with decreasing temperature. Below ~ 160 K, the calculated EF spectra are located in the low-energy side of the measured SEF spectra. Further, it has been found from the analysis of the TRF spectra that the energy relaxation time is much shorter than the excited-state lifetime at room temperature, while it increases with decreasing temperature and becomes comparable to the lifetime around 170 K. Hence it is obvious in this case that the decrease in the magnitude of the relaxation due to the increase in the relaxation time is responsible for the increase in the difference between the SEF and EF spectra with decreasing temperature.

The above spectral characteristics below ~ 160 K are very similar to those of SEF spectra of ZnMb. However, there exists a significant difference in the TRF spectra between dye solutions and ZnMb. Namely, dye solutions clearly show a time-dependent peak shift of the TRF spectrum in the temperature range where the temperature-dependent peak shift is observed in the SEF spectrum, while ZnMb does not. Next, we discuss this difference.

In the case of dye solutions, the energy relaxation in the excited state is known to be expressed approximately by a single exponential function, like the Debye-type relaxation. For example, the time-dependent shift of the peak energy $E_f(t)$ of the TRF spectrum following the relation of

$$\frac{E_f(t) - E_f(\infty)}{E_f(0) - E_f(\infty)} = \exp(-t/\tau) \quad (15)$$

has been observed for rhodamine 6G in ethanol in the temperature range where the SEF spectrum shows a temperature-dependent peak shift.²¹ It has been shown in this case that the energy relaxation time τ changes with temperature according to the Arrhenius formula

$$\tau = \frac{1}{A} \exp\left[\frac{V}{k_B T}\right], \quad (16)$$

where V is the barrier height of the relaxation and A is the frequency factor of the order of $k_B T/h$ with Planck's constant h . In this case, it is easy to show that the time-dependent peak shift of the TRF spectrum, as well as the

temperature-dependent peak shift of the SEF spectrum, is observed around the temperature where τ is comparable to the fluorescent decay time.

The TRF spectrum of ZnMb is time independent between 0.4 and 4 ns after the excitation in the temperature range where the SEF spectrum shows a temperature-dependent change due to the relaxation among the conformational substates. Thus the relaxation process of ZnMb among the substates is considered to be different from that of dye-solution systems. It should be noted that about 70% of the contribution to the SEF spectrum comes from the fluorescence in the above time range of the observation, when the decay is single exponential with a time constant of 2.1 ns. Since the SEF spectrum is obtained by the time integration of the TRF spectrum, the time dependence of the TRF spectrum should be observed at some temperature in this case, as long as the relaxation rate changes smoothly with temperature. Namely, if there is a temperature range where the time scale of the relaxation exists in the time window of the observation of the TRF spectrum, the time-dependent peak shift of the TRF spectrum, which depends on temperature, should be observed in this temperature range where the SEF spectrum is also temperature dependent.

One might consider that the above characteristics for ZnMb can be explained by a distribution of energy relaxation times. Namely, since the protein molecules are considered to have a wide distribution of energy relaxation times and also since the time range of the observation of the TRF spectrum is only one decade, the fraction of the protein molecules with their relaxation times in the time scale of the observation might be considered to be so small that the temporal variation of the TRF spectrum is not observed even in the temperature range where the SEF spectrum shows a temperature-dependent peak shift. However, this is not true, as long as the relaxation time changes smoothly with temperature. This can be confirmed by calculating the fraction of molecules whose relaxation times are in the time window of the observation, under the condition that the SEF spectrum is nearly the same as the EF spectrum at room temperature. For example, if we consider the case of an ensemble heterogeneity that each molecule in a system shows an exponential relaxation to the equilibrium state with a time constant that follows the Arrhenius relation and is different from one molecule to another, the above fraction becomes as large as ~ 0.2 .

For many relaxation processes in proteins and glasses, the temperature dependence of the average relaxation time is not Arrhenius type, but follows the Vogel-Fulcher law, Ferry law, and so on.³⁴⁻³⁶ It is known that the Ferry law can be explained by a diffusion in a rough potential with the barrier heights of a Gaussian distribution.^{37,38} It is considered that the relaxation process in a rough potential corresponds to that shown schematically in Fig. 1. In these non-Arrhenius cases, the average relaxation time varies smoothly with temperature, as in the case of the Arrhenius process. Since our results of the SEF and TRF spectra cannot be explained as long as the system has the average relaxation time changing smoothly with temperature, it is difficult to explain our results even if we consider the cases that the relaxation time obeys Vogel-Fulcher law, Ferry law, and so on.

In order to understand our experimental results, it is necessary to consider that the relaxation among the conforma-

tional substates occurs very rapidly, but the thermal equilibrium is not attained within the excited-state lifetime. The distribution of the static potential barriers with various heights does not account for the observed characteristics, though it is clear from various experimental results that a number of conformational substates separated by potential barriers are present in proteins. Further, the tunneling process is not considered to be dominant, because the magnitude of relaxation depends on temperature. Hence we come to the idea of the temperature-dependent change in the barrier height, which is not continuous with respect to temperature, contrary to the case of the Vogel-Fulcher or the Ferry relation. Namely, ZnMb is considered to relax on the potential surface of the excited state very rapidly, but only down to a certain conformational substate at a temperature and to another substate with a lower energy when temperature is increased to a certain value, mainly because of the descent of the barrier height with increasing temperature.

F. Analysis in terms of hierarchically constrained dynamics

As for the relaxation phenomena of complex systems such as glassy materials, it is known that a variety of materials show nonexponential relaxation, such as the stretched-exponential time profile in Kohlrausch anomalous relaxation law.³⁹ This behavior is usually explained by a distribution of relaxation times, namely, by a suitably weighted sum of exponential relaxations with different relaxation times. Recently, Palmer *et al.*⁴⁰ have proposed the hierarchically constrained dynamics (HCD) as a mechanism of the glassy relaxation and shown that the stretched-exponential relaxation behavior is derived on the basis of HCD. In this dynamics, the degrees of freedom of a system are divided into hierarchical groups of atoms, where the movement of a large group of atoms is constrained by some of small groups and the release of the constraint, i.e., a relaxation, occurs only when the small groups find such a combination of the configuration that makes the release possible. Thus it gives a mechanism underlying a distribution of relaxation times.

In this section we discuss our experimental results on the basis of HCD. However, since a stretched-exponential time profile was not observed in ZnMb, we do not intend to apply the theory developed by Palmer *et al.*, but focus our attention on the dynamics itself and discuss the temperature dependence of the relaxation. In this HCD model, a system has hierarchical groups of atoms and the movement of a certain size of group of atoms is triggered by the movement of smaller size of groups. Therefore, it is important that the smaller groups can find such an arrangement that realizes the release, e.g., by leaving a hole or weakening a bond. As temperature is elevated, the fluctuation of the groups of atoms becomes large. When the temperature reaches a certain value, the groups may happen to find the right arrangement and the release may occur. If we use a model of crossing over a potential barrier, this is interpreted in terms that the potential-barrier height for the relaxation of a certain size of group is influenced by the motion of the smaller size of the groups and an abrupt descent of the height occurs at a certain temperature. Conversely, below this temperature, the barrier height for the relaxation of the group remains too high for the relaxation to occur within the time scale of the observation. It is natural that the release of a larger group occurs at

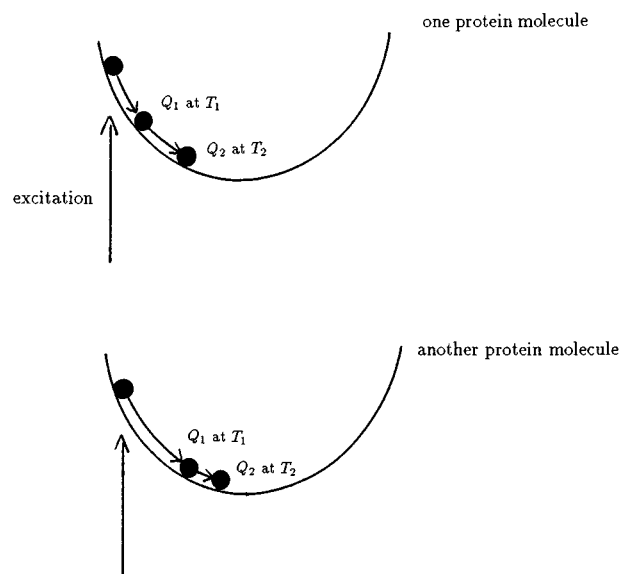


FIG. 10. Schematic picture of the relaxation due to the hierarchically constrained dynamics based on the configuration-coordinate model.

higher temperatures, because the process that the large groups find the right arrangement will require large fluctuation. Thus, as temperature is increased, the release will occur in turn from a small group to a large one. Since the release will take place suddenly at a temperature like a cooperative phenomenon, the relaxation is quite different not only from the Arrhenius type but also from the Vogel-Fulcher and Ferry types.

The overall conformation of a protein is determined by an amino acid sequence. Further, this network of the atoms is folded closely. Hence its conformational fluctuation is considered to be much constrained compared with the fluctuation of the configuration of molecules in a liquid. Further, since a protein molecule itself is considered to have a large number of degrees of freedom and a variety of time scales, i.e., a hierarchy, for the relaxation, it will be reasonable that the HCD holds for the relaxation of a single protein molecule.

If we apply the CC model, the above-mentioned dynamics will be described as seen in Fig. 10. A protein molecule excited onto the potential curve in the excited state can relax to a coordinate Q_1 on the curve at a temperature T_1 , to Q_2 at T_2 , and so on, and finally, to the bottom of the curve at T_f . Since we have assumed a one-dimensional coordinate for the conformational change, various conformational substates with the same energy may belong to the same value of Q . Further, the excited molecules in different conformational substates are considered to have different hierarchies for the relaxation modes, i.e., different distributions of triggering temperatures and partially relaxed conformations at these temperatures. Therefore, T_1, T_2, \dots and Q_1, Q_2, \dots are expected to be distributed broadly. Thus, when temperature is increased, the distribution of the ensemble of proteins on the potential curve will broaden and the center of gravity of the distribution will shift toward the bottom of the potential curve. Then, the peak energy of the SEF spectrum shows a

redshift and its width broadens as temperature is increased. However, the time-dependent change of the TRF spectrum is not observed if the movement on the potential curve occurs much faster than the temporal resolution of our measurement at each temperature. Further, if T_f 's are not lower than room temperature, the excitation-energy dependence of the SEF spectrum will be observed up to room temperature because the protein molecules do not reach the thermal equilibrium state in the excited state. Thus the whole experimental results on ZnMb can be explained qualitatively by this model.

Next, we simulate the temperature dependence and the excitation-energy dependence of the SEF spectrum on the basis of this model. Although there will be many steps for the relaxation as described above, only two steps are taken into account in this simulation. Namely, we assume that the molecule excited onto the potential curve at Q_{ex} relaxes to Q_1 at T_1 and reaches the equilibrium conformation at T_2 . If we take into account the broad distributions of Q_1 , T_1 , and T_2 , this simple model may reproduce the relaxation dynamics due to the above model rather correctly. We further assume that T_1 's are low compared to the temperature range of our measurement, so that the relaxation step to Q_1 already finishes within the temporal resolution of our measurement even at the lowest temperature examined. Further, it is also assumed that T_2 is distributed and the fraction of the population in the thermal equilibrium changes linearly with temperature according to

$$\frac{N_{\text{eq}}(T)}{N} = \frac{T - T_s}{T_e - T_s}, \quad (17)$$

where N is the total number of the population in the excited state and T_s and T_e are suitable temperatures. On the other hand, the nonthermalized population is assumed to be distributed uniformly, on account of the distribution of Q_1 , between Q_{ex} and Q_0 , which corresponds to the bottom of the potential curve, at each temperature. Then, using the same CC model as in the previous sections, the population distributions of the nonthermalized molecules $P_{\text{nonth}}(Q)$ and the molecules in the thermal equilibrium $P_{\text{eq}}(Q)$ are given as

$$P_{\text{nonth}}(Q) = \begin{cases} [N - N_{\text{eq}}(T)](Q_0 - Q_{\text{ex}})^{-1}, & Q_{\text{ex}} \leq Q \leq Q_0 \\ 0 & \text{otherwise} \end{cases} \quad (18)$$

and

$$P_{\text{eq}}(Q) = N_{\text{eq}}(T) \sqrt{\frac{a}{\pi k_B T}} \exp\left[-\frac{a(Q - Q_0)^2}{k_B T}\right], \quad (19)$$

respectively.

The shape function of the SEF spectrum is expressed as

$$I^{\text{SEF}}(\omega, \omega_l) = \int_0^\infty G'_T(\omega_0) f^{\text{fl}}(\omega - \omega_0) d\omega_0, \quad (20)$$

where $G'_T(\omega_0)$ is the site-energy distribution function in the excited state at T and is given from Eq. (5) as

$$G'_T(\omega_0) = \int_{-\infty}^\infty \{P_{\text{nonth}}(Q) + P_{\text{eq}}(Q)\} \delta[\omega_0 - \Delta U(Q)] dQ. \quad (21)$$

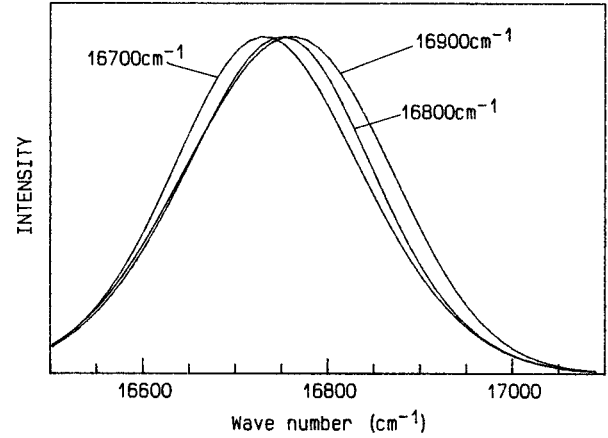


FIG. 11. Excitation-energy dependence of the SEF spectrum at 293 K calculated from Eq. (22). The parameters employed are $d = 37 \text{ cm}^{-1}$, $\Delta_s = 25 \text{ cm}^{-1}$, $T_s = 150 \text{ K}$, and $T_e = 320 \text{ K}$.

Employing a high-temperature approximation, for simplicity, we regard the single-site fluorescence spectrum as a Gaussian.²⁶ Then, we obtain

$$\begin{aligned} I^{\text{SEF}}(\omega, \omega_l) &= \frac{N - N_{\text{eq}}(T)}{\omega_l - (E - d)} \\ &\times \int_{E-d}^{\omega_l} \exp\left[-\frac{(\omega - \omega_0 + \Delta_s/2)^2}{2k_B T \Delta_s}\right] d\omega_0 \\ &+ N_{\text{eq}}(T) \sqrt{\frac{\Delta_s}{\Delta_s + d}} \\ &\times \exp\left[-\frac{(\omega - E + \Delta_s/2 + d)^2}{2k_B T (\Delta_s + d)}\right], \quad (22) \end{aligned}$$

where Δ_s is the energy difference between the peak energies of the single-site absorption and fluorescence spectra. It should be noted that it is not necessary to consider the effect of the conformational relaxation dynamics in the calculation of the fluorescence spectrum, because the fast relaxation is completed within a time much shorter than the fluorescent decay time. Figure 11 shows the excitation-energy dependence of the SEF spectrum obtained from Eq. (22). It was found that the temperature dependence of the single-site fluorescence spectrum calculated from the WDOS can be roughly reproduced by the fluorescence spectrum under a high-temperature approximation with Δ_s of 25 cm^{-1} . Hence this value was used for Δ_s in this simulation. In Fig. 11 the peak energy of the simulated spectrum shows an excitation-energy dependence, which is very similar to the experimental result. Next, the simulated temperature dependence of the SEF spectrum is shown in Fig. 12. The temperature dependence of E obtained from the analysis of the absorption spectrum was employed. The fluorescence spectrum shows the peak shift toward the low-energy side and broadening with increasing temperature. These features agree with the experimental results very well. Thus we can say that the whole experimental results can be explained by our model in which the essential idea underlying the hierarchically constrained dynamics has been used.

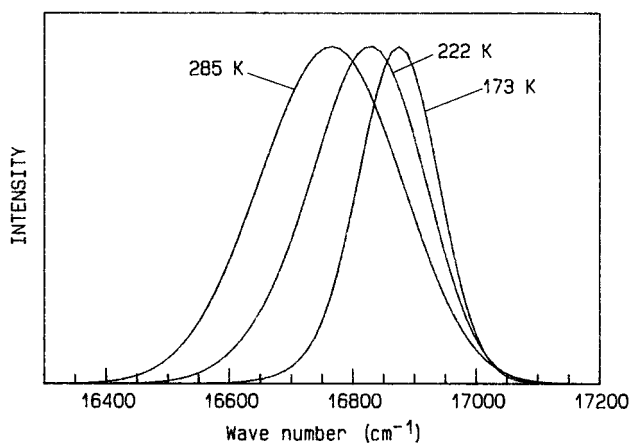


FIG. 12. Temperature dependence of the SEF spectrum calculated from Eq. (22). The excitation wave number is $16\,940\text{ cm}^{-1}$ and the parameters are the same as in Fig. 11.

Proteins, as observed in ligand binding kinetics of myoglobin, often exhibit slow dynamics that are nonexponential in time.¹⁷ If the excited-state lifetime were long enough in ZnMb, each protein molecule would be able to cross the high potential barriers in the excited state and the system may show a nonexponential slow relaxation on account of the ensemble heterogeneity. However, since our time window of observation is limited by the short lifetime of the excited state, the slow relaxations are not concerned with our experimental results. Nonexponential relaxations that are not explainable as the Arrhenius process have been observed in slow dynamics in glasses and proteins.^{41,42} To our knowledge, however, our experiment is the first case that this type

of relaxation dynamics has been observed in a very short time range and also in the electronic excited state. Further, our results cannot be explained by the distribution of the time constant of the relaxation to the equilibrium state, but are considered to be explained only by a distribution of triggering temperatures for the relaxation to partially relaxed states.

VI. CONCLUSION

A protein molecule is a typical complex system and shows glasslike features. We have investigated the energy relaxation process in the excited state of Zn-substituted myoglobin from 170 K to room temperature by laser-excited fluorescence spectroscopy. It has been found that this protein shows a conformational relaxation that finishes within a few hundred picoseconds and the magnitude of the relaxation becomes larger with increasing temperature. This relaxation is very different from that of dye solutions and is not accounted for by the thermal crossing of static potential barriers. The experimental results have been explained using a model based on the hierarchically constrained dynamics. We believe that this relaxation dynamics reflects the features of a protein molecule as a complex system.

ACKNOWLEDGMENTS

The authors are indebted to Y. Kanematsu, J.S. Ahn, and E. Enomoto for valuable discussions, suggestions, and offering the data of the WDOS of ZnMb. They are grateful to S. Kinoshita and A. Kurita for fruitful discussions and to K. Hirata for helpful advice in preparing the samples. The authors gratefully acknowledge the support by the Research Foundation for Opto-Science and Technology.

¹H. Frauenfelder, F. Parak, and R. D. Young, *Annu. Rev. Biophys. Chem.* **17**, 451 (1988).

²H. Frauenfelder, G. A. Petsko, and D. Tsernoglou, *Nature* **280**, 558 (1979).

³H. Hartmann, F. Parak, W. Steigemann, G. A. Petsko, D. Ringepozzi, and H. Frauenfelder, *Proc. Natl. Acad. Sci. U.S.A.* **79**, 4967 (1982).

⁴F. Parak, H. Hartmann, K. D. Aumann, H. Reuscher, G. Rennekamp, H. Bartunik, and W. Steigemann, *Eur. Biophys. J.* **15**, 237 (1987).

⁵F. Parak and H. Formanek, *Acta Crystallogr. Sec. A* **27**, 573 (1971).

⁶F. Parak, E. N. Frolov, A. A. Kononenko, R. L. Mössbauer, V. I. Goldanskii, and A. B. Rubin, *FEBS Lett.* **117**, 368 (1980).

⁷H. Keller and P. G. Debrunner, *Phys. Rev. Lett.* **45**, 68 (1980).

⁸F. Parak, E. N. Frolov, R. L. Mössbauer, and V. I. Goldanskii, *J. Mol. Biol.* **145**, 825 (1981).

⁹S. G. Cohen, E. R. Bauminger, I. Nowik, S. Ofer, and J. Yariv, *Phys. Rev. Lett.* **46**, 1244 (1981).

¹⁰F. Parak, P. Finck, D. Kucheida, and R. L. Mössbauer, *Hyperfine Interact.* **10**, 1075 (1981).

¹¹G. P. Singh, H. J. Schink, H. V. Löhneysen, F. Parak, and S. Hunklinger, *Z. Phys. B* **55**, 23 (1984).

¹²A. Schulte and R. Murray, *Phys. Rev. B* **36**, 1772 (1987).

¹³Y. Miyazaki, T. Matsuo, and H. Suga, *Chem. Phys. Lett.* **213**, 303 (1993).

¹⁴W. Doster, S. Cusack, and W. Petry, *Nature* **337**, 754 (1989).

¹⁵W. Doster, S. Cusack, and W. Petry, *J. Non-Cryst. Solids* **131-133**, 357 (1991).

¹⁶F. Parak and H. Frauenfelder, *Physica A* **201**, 332 (1993).

¹⁷R. H. Austin, K. W. Beeson, L. Eisenstein, H. Frauenfelder, and I. C. Gunsalus, *Biochem.* **14**, 5355 (1975).

¹⁸A. Ansari, J. Berendzen, S. F. Bowne, H. Frauenfelder, I. E. T. Iben, T. B. Sauke, E. Shyamsunder, and R. D. Young, *Proc. Acad. Natl. Sci. U.S.A.* **82**, 5000 (1985).

¹⁹T. Kushida, J. S. Ahn, K. Hirata, and A. Kurita, *Biochem. Biophys. Res. Commun.* **160**, 948 (1989).

²⁰S. Kinoshita, N. Nishi, and T. Kushida, *Chem. Phys. Lett.* **134**, 605 (1987).

²¹S. Kinoshita and N. Nishi, *J. Chem. Phys.* **89**, 6612 (1988).

²²J. S. Ahn, Y. Kanematsu, and T. Kushida, *Chem. Phys. Lett.* **215**, 336 (1993).

²³H. Murakami and T. Kushida, *J. Lumin.* **58**, 172 (1994).

²⁴S. Kinoshita, N. Nishi, A. Saitoh, and T. Kushida, *J. Phys. Soc. Jpn.* **56**, 4162 (1987).

²⁵H. Murakami, S. Kinoshita, Y. Hirata, T. Okada, and N. Mataga, *J. Chem. Phys.* **97**, 7881 (1992).

- ²⁶S. Nakajima, Y. Toyozawa, and R. Abe, *The Physics of Elementary Excitations* (Springer-Verlag, Berlin, 1980), p. 263.
- ²⁷J. S. Ahn, Y. Kanematsu, and T. Kushida, *Phys. Rev. B* **48**, 9058 (1993).
- ²⁸Y. Kanematsu, J. S. Ahn, and T. Kushida, *Phys. Rev. B* **48**, 9066 (1993).
- ²⁹M. Gouterman, in *The Porphyrins*, edited by D. Dolphin (Academic, New York, 1978), Vol. 3, p. 1.
- ³⁰S. Kinoshita and T. Kushida, *Anal. Instrum.* **14**, 503 (1985).
- ³¹Y. Ooshika, *J. Phys. Soc. Jpn.* **9**, 594 (1954).
- ³²J. Watanabe, H. Takahashi, J. Nakahara, and T. Kushida, *Chem. Phys. Lett.* **213**, 351 (1993).
- ³³J. Watanabe, J. Nakahara, and T. Kushida, *J. Lumin.* **58**, 194 (1994).
- ³⁴G. S. Fulcher, *J. Am. Ceram. Soc.* **8**, 339 (1925).
- ³⁵M. L. Williams, R. F. Landel, and J. D. Ferry, *J. Am. Ceram. Soc.* **77**, 3701 (1953).
- ³⁶P. J. Steinbach, A. Ansari, J. Berendzen, D. Braunstein, K. Chu, B. R. Cowen, D. Ehrenstein, H. Frauenfelder, J. B. Johnson, D. C. Lamb, S. Luck, J. R. Mourant, G. U. Nienhaus, P. Ormos, R. Philipp, A. Xie, and R. D. Young, *Biochemistry* **30**, 3988 (1991).
- ³⁷R. Zwanzig, *Proc. Natl. Acad. Sci. U.S.A.* **85**, 2029 (1988).
- ³⁸R. Richert and H. Bässler, *J. Phys.: Condens. Matter* **2**, 2273 (1990).
- ³⁹K. L. Ngai, *Comments Solid State Phys.* **9**, 141 (1980).
- ⁴⁰R. G. Palmer, D. L. Stein, E. Abrahams, and P. W. Anderson, *Phys. Rev. Lett.* **53**, 958 (1984).
- ⁴¹J. Jäckle, *Rep. Prog. Phys.* **49**, 171 (1986).
- ⁴²I. E. T. Iben, D. Braunstein, W. Doster, H. Frauenfelder, M. K. Hong, J. B. Johnson, S. Luck, P. Ormos, A. Shulte, P. J. Steinbach, A. Xie, and R. D. Young, *Phys. Rev. Lett.* **62**, 1916 (1989).